



UNIVERSITY OF LEEDS

This is a repository copy of *Efficacy of epsilon-poly-L-lysine inhibition of postharvest blue mold in apples and potential mechanisms*.

White Rose Research Online URL for this paper:  
<https://eprints.whiterose.ac.uk/180561/>

Version: Accepted Version

---

**Article:**

Dou, Y, Routledge, MN, Gong, Y [orcid.org/0000-0003-4927-5526](https://orcid.org/0000-0003-4927-5526) et al. (5 more authors) (2021) Efficacy of epsilon-poly-L-lysine inhibition of postharvest blue mold in apples and potential mechanisms. *Postharvest Biology and Technology*, 171. 111346. p. 111346. ISSN 0925-5214

<https://doi.org/10.1016/j.postharvbio.2020.111346>

---

© 2020 Elsevier B.V. All rights reserved. This manuscript version is made available under the CC-BY-NC-ND 4.0 license <http://creativecommons.org/licenses/by-nc-nd/4.0/>.

**Reuse**

This article is distributed under the terms of the Creative Commons Attribution-NonCommercial-NoDerivs (CC BY-NC-ND) licence. This licence only allows you to download this work and share it with others as long as you credit the authors, but you can't change the article in any way or use it commercially. More information and the full terms of the licence here: <https://creativecommons.org/licenses/>

**Takedown**

If you consider content in White Rose Research Online to be in breach of UK law, please notify us by emailing [eprints@whiterose.ac.uk](mailto:eprints@whiterose.ac.uk) including the URL of the record and the reason for the withdrawal request.



[eprints@whiterose.ac.uk](mailto:eprints@whiterose.ac.uk)  
<https://eprints.whiterose.ac.uk/>



16 **Abstract:** *Penicillium expansum* is a major postharvest fungal pathogen and is the causal  
17 agent of blue mold decay in apples. Epsilon-poly-L-lysine ( $\epsilon$ -PL) is a naturally-occurring  
18 polypeptide that has strong antimicrobial activity. It is primarily used to suppress foodborne  
19 pathogens in bread, beverage, meat products, etc. The potential application of  $\epsilon$ -PL in the  
20 management of fungal postharvest diseases of fruit, however, has not been explored. In the  
21 present study, the inhibitory effect of  $\epsilon$ -PL against blue mold (*P. expansum*) disease of apples  
22 and its potential mechanism of action were investigated. Results indicated that 600 mg L<sup>-1</sup> of  
23  $\epsilon$ -PL could effectively inhibit mycelial growth of *P. expansum* in apples. Concentrations of  
24  $\epsilon$ -PL > 200 mg L<sup>-1</sup> also inhibited germination of conidia and germ tube growth of *P.*  
25 *expansum* in potato dextrose broth (PDB). The inhibitory effect increased with increasing  
26 concentrations of  $\epsilon$ -PL concentration. Further studies indicated that the possible mechanisms  
27 involved of  $\epsilon$ -PL inhibition of *P. expansum* included the activation of defense-related enzyme  
28 activity and gene expression in apple fruit tissues. This included polyphenol oxidase (PPO),  
29 catalase (CAT), peroxidase (POD) and phenylalanine ammonialyase (PAL).  $\epsilon$ -PL stimulated  
30 the production of intracellular reactive oxygen species (ROS) and degraded the integrity of  
31 the cell wall and plasma membrane of conidia, resulting in the death of conidial spores of *P.*  
32 *expansum* or their germination.

33 **Key Words:** Apple; Blue mold; Induced resistance; Epsilon-poly-L-lysine; Membrane  
34 integrity; ROS

## 35 **1. Introduction**

36 Postharvest infection of fruit by decay fungi is a global problem that results in a  
37 significant amount of economic losses annually (Zhang, et al., 2017). Blue mold disease,

38 caused by *P. expansum*, is a major postharvest disease of apple (Errampalli, 2014). Chemical  
39 fungicides are conventionally used to inhibit postharvest fungal diseases of apples, but  
40 long-term use of chemical fungicides may lead to fungicide resistance in pathogens and  
41 environmental pollution (Salomao, et al., 2008; Sansone et al., 2005; Sharma et al., 2009;  
42 Förster et al., 2007). Hence, it is important to develop effective, non-toxic, and  
43 environmentally-friendly alternatives to manage postharvest apple diseases.

44  $\epsilon$ -PL is a polypeptide consisting of 25-35 lysine residues linked by peptide bonds,  
45 formed by the dehydroxylation of the carboxyl group on the  $\alpha$ -carbon atom of one lysine and  
46 the dehydrogenation of the amino group on the  $\epsilon$ -carbon atom of another lysine (Pandey &  
47 Kumar, 2014; Shima & Sakai, 1977). The degree of antimicrobial activity of  $\epsilon$ -PL is related  
48 to its molecular weight (MW). Notably,  $\epsilon$ -PL with a MW of 3600 to 4300 Da can  
49 significantly inhibit the growth of microorganisms, while  $\epsilon$ -PLs with a MW lower than 1300  
50 Da do not exhibit antimicrobial activity (Tuersuntuoheti et al., 2019). As a natural  
51 preservative originally discovered in *Streptomyces albulus*, synthesized  $\epsilon$ -PL is safer than  
52 other chemical antimicrobials because it can be completely decomposed into lysine in the  
53 human body, an essential amino acid in humans (Bhattacharya et al., 2018; Li et al., 2014ab).  
54 No histopathological or carcinogenic effects were observed in rats when a high concentration  
55 of  $\epsilon$ -PL (20 g kg<sup>-1</sup>) added to their diet (Hosomi et al., 2015). In fact, many countries,  
56 including Japan, the USA, and South Korea currently allow the use of  $\epsilon$ -PL as a food  
57 preservative based on its antimicrobial efficacy, stability, and safety (Ye et al., 2013; Zhang et  
58 al., 2015).

59 The inhibitory effect of  $\epsilon$ -PL on foodborne pathogenic bacteria has been widely studied.  
60  $\epsilon$ -PL effectively inhibits gram-positive microbes such as *Bacillus subtilis*, *Micrococcus luteus*,  
61 and *Staphylococcus aureus*, and even more effectively inhibits gram-negative microbes such  
62 as *Salmonella typhimurium*, *Pseudomonas* spp. and *Escherichia coli* O157:H7 (Zhang et al.,  
63 2018; Hyldgaard et al., 2014). Previous studies have reported that  $\epsilon$ -PL can inhibit  
64 postharvest diseases of jujube, citrus, tomato, and kiwifruit (Li et al., 2019; Liu et al., 2017;  
65 Sun et al., 2018; Li et al., 2017b). No studies are available, however, on the ability of  $\epsilon$ -PL to  
66 control postharvest blue mold disease in apples. The purpose of the present study was to  
67 determine the ability of  $\epsilon$ -PL to inhibit blue mold disease in apples and explore the potential  
68 mechanism of action of  $\epsilon$ -PL against *P. expansum* both *in vitro* and *in vivo*. Results of the  
69 study contribute to sustainable agricultural production and the goal of replacing chemical  
70 fungicides with organic compounds for the control and prevention of postharvest diseases of  
71 perishable fruit commodities.

## 72 **2. Material and methods**

### 73 *2.1. Pathogen*

74 *P. expansum* was isolated from decayed apple tissue, and cultured as described by  
75 Zheng et al. (2017). *P. expansum* conidia were collected and preserved in an ultra-freezer at  
76 -80 °C. Prior to use in the present study, the pathogen was activated by culturing spores in  
77 PDB medium at 25 °C and 150 rpm for 24 h. The conidial suspension was subsequently  
78 spread on potato dextrose agar (PDA) and incubated at 25 °C for 7 d. After 7 d of incubation,  
79 a *P. expansum* spore suspension was prepared by adding sterile physiological saline to the  
80 plate and gently scraping conidia from the culture surface with the use of a sterile pipette

81 head. A hemocytometer was used to determine the concentration of the spore suspension and  
82 sterile normal saline was used to dilute the spore suspension to the required concentration.

### 83 2.2. *Apple fruit*

84 Mature apples (*Malus × domestica* Borkh, cv. Fuji) that had not received any chemical  
85 treatments were harvested from a fruit orchard in Yantai, Shandong province, China. Apples  
86 selected for use in the experiments were uniform in maturity and size, and free of any  
87 mechanical or pest damage. Apples were refrigerated at 4 °C immediately after picking.  
88 Apples were soaked in 0.1 % (v/v) sodium hypochlorite for 2 min before each experiment to  
89 decrease or eliminate surface microbes, rinsed with sterile water, and air-dried (Mahunu et al.,  
90 2018).

### 91 2.3. *ε-PL inhibition of blue mold in apples*

92 The effect of ε-PL on postharvest blue mold of apples was assessed as described by Li et  
93 al. (2019) and Ge et al. (2018). Selected apples were administered small wounds at the  
94 equator of each apple. Four wounds (5 mm diameter × 3 mm depth) were made with a  
95 sterilized cork borer at room temperature. Thirty μL of various concentrations (100, 200, 400,  
96 600, or 800 mg L<sup>-1</sup>) of ε-PL were administered into each wound. Sterilized saline solution  
97 was used as the control. The apples were placed in plastic containers previously sterilized  
98 with ethanol, wrapped in polyethylene film and placed in a constant temperature chamber at  
99 20 °C at 95 % relative humidity (RH). After 24 h, 30 μL of a conidial suspension (1 × 10<sup>5</sup>  
100 spores mL<sup>-1</sup>) of *P. expansum* was pipetted into each wound. The apples were then returned to  
101 the same storage conditions for six days. Decay incidence and lesion diameter were evaluated  
102 every 24 h. Each treatment consisted of three replications and each replication contained six

103 apples and four wounds per apple. The percentage of decay incidence for each replicate was  
104 calculated as follows: number of decayed wounds/total number of wounds  $\times$  100. The lesion  
105 diameter for each replicate was calculated by measuring the average diameter of all the rotten  
106 wounds. The whole experiment was carried out twice.

#### 107 *2.4. Effect of $\epsilon$ -PL on *P. expansum* mycelial growth in apples*

108 Thirty  $\mu$ L of 600 mg L<sup>-1</sup>  $\epsilon$ -PL was administered in wounds of apple as previously  
109 described, with sterilized saline solution used as a control, to study the effect of  $\epsilon$ -PL on  
110 mycelial growth in apple tissues. Thirty  $\mu$ L of a conidial suspension ( $1 \times 10^5$  spores mL<sup>-1</sup>)  
111 was subsequently added into each wound after the apples were stored at 20 °C and 95 % RH  
112 for 24 h. The treated apples were then packed as previously described and returned to storage  
113 conditions for up to 18 h. Tissue samples were collected from the apple wounds at 9 h, 12 h,  
114 and 18 h and prepared for scanning electron microscopy (SEM). The wounded tissue samples  
115 were cut into thin slices approximately 1 mm thick with a sterile razor blade and then placed  
116 in 2.5 % glutaraldehyde solution at 4 °C for more than 4 h. Samples were then rinsed with 0.1  
117 M phosphate buffer system (PBS) pH 7.2 for 1 min. The apple tissue slices were then passed  
118 through a series of increasing concentrations of ethanol (30 %, 50 %, 70 %, 90 %), allowing  
119 them to stay in each solution for at least 5 min (Pietrysiak et al., 2018; Daniel et al., 2015).  
120 Samples were then immediately vacuum freeze-dried for 24 h, and attached to a conductive  
121 metal grid, coated with gold/palladium and viewed on a field emission scanning electron  
122 microscope (JSM-7001F, JEOL, Japan).

#### 123 *2.5. Effect of $\epsilon$ -PL on the morphology of *P. expansum* mycelia in vitro*

124 Morphological alterations in the mycelia of *P. expansum* were examined using SEM as  
125 described by He et al. (2011). Samples of  $1 \times 10^5$  spores  $\text{mL}^{-1}$  were cultured for 9 h at 25 °C  
126 and 150 rpm in PDB media amended with  $\epsilon$ -PL (0, 200, 400, or 600  $\text{mg L}^{-1}$ ). Cultures were  
127 then centrifuged for 3 min at  $8000 \times g$  and the precipitates were collected and rinsed with  
128 PBS. The collected mycelia were then fixed in 2.5 % glutaraldehyde and dehydrated in  
129 ethanol as previously describe. Mycelial samples were then placed on a rectangular cover  
130 glass of size 3 mm  $\times$  6 mm, and the cover glass was attached to a conductive grid pasted with  
131 conductive adhesive. The samples were then dried for 24 h using a vacuum freeze-dryer and  
132 coated with gold/palladium. Morphological alterations in the mycelia caused by exposure to  
133 the  $\epsilon$ -PL were observed using SEM.

#### 134 2.6. Intracellular ROS determination and plasma membrane integrity

135 Intracellular ROS and plasma membrane integrity of *P. expansum* spores were examined  
136 as previously described (Su et al., 2018; Li et al., 2017a; Shi et al., 2012). Briefly, conidia of  
137 *P. expansum* were cultured in PDB media amended with various concentration of  $\epsilon$ -PL (0,  
138 200, and 400  $\text{mg L}^{-1}$ ) for 9 h at a constant temperature of 25 °C on a rotary shaker set at 150  
139 rpm. The conidial cultures were then centrifuged for 3 min at  $8000 \times g$  at room temperature.  
140 The conidia were washed twice with PBS. The centrifuged samples of conidia were then  
141 stained with 10  $\mu\text{M}$  of 2',7'-dichlorodihydro fluorescein diacetate (DCFH-DA), and 10  $\text{mg L}^{-1}$   
142 propidium iodide (PI) solutions. Samples were placed in a shaking incubator at 30 °C and  
143 150 rpm for 30 min in dark. The conidia and germ tubes were then immediately observed  
144 under a fluorescence microscope. Three fields of view with about 100 conidia were randomly

145 selected to take pictures, and the ratio of the number of conidia producing ROS and the  
146 number of conidia with cell leakage to the total number of conidia was calculated.

## 147 *2.7. Examination of cellular leakage in P. expansum*

148 Leakage of cellular contents from *P. expansum* mycelia was examined as described by  
149 Cai et al. (2015), Cui et al. (2018), and Zhu et al. (2019). *P. expansum* spores were on PDA  
150 media for 7 d. Conidia were then collected from the PDA plate and spore concentration was  
151 adjusted to  $1 \times 10^5$  spores mL<sup>-1</sup> with sterile saline solution and the aid of a hemocytometer.  
152 The collected conidia were cultured in PDB medium on a shaking incubator at 150 rpm and  
153 25 °C for 72 h. Samples of the cultures were then collected and washed with sterile distilled  
154 water. The washed mycelia were resuspended in 100 mL of various concentrations ε-PL (0,  
155 200, and 400 mg L<sup>-1</sup>), and cultured at 25 °C for 1, 2, 3, and 4 h on a rotary shaker set at 150  
156 rpm. The mycelial suspensions were then centrifuged for 3 min at 8000 × g. The resulting  
157 supernatants were used to assay the level of soluble proteins and nucleic acids which would  
158 be indicative of cell leakage. The Bradford assay (Bradford, 1976) was used to quantify  
159 soluble proteins. The concentration of nucleic acids was determined by measuring  
160 absorbance at 260 nm ( $A_{260\text{nm}}$ ). Three replicates were used for each treatment and the  
161 experiment was repeated twice.

## 162 *2.8. Analysis of enzyme activity and corresponding gene expression in apples*

### 163 *2.8.1. Defense-related enzyme activity*

164 Apple samples were surface sterilized and artificially wounded as previously described.  
165 Thirty μL of 600 mg L<sup>-1</sup> ε-PL was then administered into each wound, with sterile saline  
166 used as a control. The apples were placed in plastic container wrapped in polyethylene film

167 and stored at 20 °C and 95 % RH. Apple tissues surrounding the wounds were collected and  
168 mixed at 0, 1, 2, 3, 4, 5, 6, and 7 d after treatment. The mixed tissue samples were divided  
169 into two parts, one portion of the samples was immediately frozen in liquid nitrogen and kept  
170 at -80 °C for subsequent determination of defense-related gene expression, and the other  
171 portion was used to assay defense-related enzyme activity. Each treatment consisted of three  
172 replications and each replication contained six apples and four wounds per apple.

173 Tissue samples (about 2 g) and a little silica sand were placed together in a pre-frozen  
174 mortar and ground in 1 mL precooled PBS (50 mM, pH 7.8) with 0.038 % ethylene  
175 diaminetetraacetic acid and 1 % polyvinylpyrrolidone. The ground apple tissue samples were  
176 then transferred to a centrifuge tube and washed by adding 9 mL of PBS, and centrifuged at  
177  $12000 \times g$  for 8 min at 4 °C (Zhao et al., 2020). The enzyme activity of PAL, POD, PPO, and  
178 CAT in the collected supernatant was determined following the protocols described in  
179 Apaliya et al. (2017), Wang et al. (2019), and Wang et al. (2018). All the apple tissue weight  
180 mentioned in this paper refer to the fresh weight. Enzyme activity is indicated as U g<sup>-1</sup> fresh  
181 weight of samples.

182 PAL activity was determined as described by Wang et al. (2019) with some  
183 modifications. Crude enzyme extract (1mL) was added into 3 mL, 50 mM borate buffer  
184 solution (pH 8.8, preheated at 37 °C for 5 min) containing 10 mM phenylalanine. The initial  
185 absorbance value was measured at 290 nm and the test time was accurately recorded. One mL  
186 of 50 mM PBS (pH 7.8) was used as the blank. The absorbance values of the samples and  
187 control were measured again after 1 h at 290 nm. PAL enzyme activity was calculated by

188 subtracting the two absorbance values. One unit of PAL activity was defined as an increase of  
189 0.01 absorbance unit per hour at 290 nm.

190 POD activity was determined according to Apaliya et al. (2017) with some  
191 modifications. Crude enzyme extract (0.2 mL) was added into 2.2 mL, 50 mM PBS (pH 6.4,  
192 containing 0.3 % guaiacol). Then 0.6 mL of 0.3 % H<sub>2</sub>O<sub>2</sub> (50 mM PBS, pH 6.4) was added  
193 and samples were incubated at 30 °C for 6 min. POD activity was determined by measuring  
194 absorbance at 470 nm every 60 s for 3 min. The blank control consisted of 0.2 mL 50 mM  
195 PBS (pH 6.4). POD activity was determined by and increase of 0.01 absorbance unit per  
196 minute at 470 nm.

197 PPO activity was measured according to the method previously described by Wang et al.  
198 (2018) with some modifications. The reaction mixture was composed of 0.2 mL crude  
199 enzyme extract and 2.8 mL pyrocatechol of 0.1 mM (50 mM PBS, pH 6.4) and was incubated  
200 at 30 °C for 6 min. POD activity was determined by measuring absorbance at 398 nm every  
201 60 s for 3 min. The blank control was the same one used in the POD assay. PPO activity was  
202 calculated based on an increase of 0.01 absorbance unit per minute at 398 nm.

203 CAT activity was determined according to Wang et al. (2019) with some modifications.  
204 Crude enzyme extract (0.2 mL) was added into 2.8 mL H<sub>2</sub>O<sub>2</sub> of 30 mM (50 mM PBS, pH  
205 7.8). Absorbance was recorded 240 nm every 60 s for 3 min. The blank control was the same  
206 one used in the POD assay. One unit of CAT activity was defined as a decrease of 0.01  
207 absorbance unit per minute at 240 nm.

208 *2.8.2. Reverse transcription - quantitative polymerase chain reaction (RT-qPCR) analysis of*  
209 *defense-related gene expression*

210 Frozen apple tissue (2 g) stored at -80 °C was used to extract RNA with a plant total  
211 RNA purification kit (Sangon Biotech, Shanghai, China) according to the manufacturer's  
212 instructions. Absorbance at 260 and 280 nm measured in a spectrophotometer was used to  
213 evaluate the purity and quantity of RNA. The integrity and content of RNA was determined  
214 using and RNA Nano 6000 assay kit and a Bioanalyzer 2100 system (Agilent Technologies,  
215 CA, USA). First strand cDNA was synthesized from total RNA using a PrimeScript RT  
216 reagent kit and gDNA Eraser (Takara-Dalian, China). Specific primers for the evaluated  
217 genes were designed with Primer Premier 5.0 software (PREMIER Biosoft International,  
218 Palo Alto, CA, USA) and listed in Table 1. RT-qPCR was performed with a Biorad CFX96  
219 Real Time PCR System (Applied Biosystems, USA). The PCR conditions were the same as  
220 those described in Wang et al. (2019). Amplification products have tested the specificity  
221 in accordance with the melting curve analysis was used to evaluate the specificity of the  
222 primers used to generate the amplification products. RT-qPCR was carried out using TB  
223 Green® Fast qPCR Mix (TAKARA BIO Inc., Shiga, Japan) in an ABI PRISM 7500  
224 Real-Time PCR System (Applied Biosystems, USA) according to the manufacturer's  
225 instructions. The amplification protocol was 95 °C for 15 s, 60 °C for 1 min, 95 °C for 15 s,  
226 and 62 °C for 15 s. Relative gene expression levels was determined using  $2^{-\Delta\Delta CT}$  method  
227 using the Ct value of apple *Actin* for normalization (Livak and Schmittgen, 2001). The  
228 RT-qPCR analysis was conducted for three biological and technical replicates.

### 229 2.9. Statistical analysis of data

230 Each treatment consisted of three biological replicates and all the experiments were  
231 repeated at least twice. Analysis of variance (ANOVA) was carried out using SPSS 22.0

232 software (SPSS Inc., Chicago, IL, USA). Tukey's test was used for means separations, and  $P$   
233  $< 0.05$  was considered as statistically significant.

### 234 **3. Results**

#### 235 *3.1. Inhibitory effect of $\epsilon$ -PL on blue mold in apples*

236 Inhibitory effect of  $\epsilon$ -PL on blue mold infection of apples varied with the concentration  
237 of  $\epsilon$ -PL (Fig. 1). Decay incidence and lesion diameter in the 100 mg L<sup>-1</sup>  $\epsilon$ -PL treatment was  
238 not significantly different from the control, indicating that lower concentrations of  $\epsilon$ -PL were  
239 ineffective against the growth of blue mold in apples. In contrast, decay incidence and lesion  
240 diameter decreased significantly with the use of  $\epsilon$ -PL concentration ranging from 200 to 800  
241 mg L<sup>-1</sup>. Notably, a major decrease was observed in the 600 mg L<sup>-1</sup> treatment group. While  
242 results indicated that 600 mg L<sup>-1</sup>  $\epsilon$ -PL exhibited the greatest ability to inhibit blue mold, use  
243 of a  $\epsilon$ -PL concentration of 800 mg L<sup>-1</sup>, decay incidence and decay diameter significantly  
244 increased above the 600 mg L<sup>-1</sup>  $\epsilon$ -PL. This suggests that highest concentration of  $\epsilon$ -PL may  
245 have been cytotoxic to apples.

#### 246 *3.2. Effect of $\epsilon$ -PL on *P. expansum* mycelial growth in vivo*

247 As shown in Fig. 2, SEM observations revealed that  $\epsilon$ -PL significantly inhibited the  
248 growth of *P. expansum* in apple tissues. The conidia of *P. expansum* in the wounds of the  
249 control group began to germinate after 12 h, and elongated germ tubes were clearly evident.  
250 Later observations of the control group indicated that the fungus readily grew in the wounded  
251 tissues as evidenced by the copious amounts of visible mycelia. In contrast, germination of  
252 conidia in the  $\epsilon$ -PL-treated wounds was not observed until at least 18 h after inoculation, and  
253 the surface of conidia appeared shriveled and shrunken. These results indicate that the conidia

254 in the  $\epsilon$ -PL-treated wounds were under stress and may have been subject to a loss of cellular  
255 integrity, thus resulting in an inhibition of mycelial growth.

### 256 3.3. Effect of $\epsilon$ -PL on the morphology of *P. expansum* mycelia in vitro

257 The morphology of mycelia and germ tubes of *P. expansum* treated with  $\epsilon$ -PL were  
258 observed using SEM. *P. expansum* conidia that were not treated with  $\epsilon$ -PL germinated and  
259 developed germ tubes that had a smooth surface (Fig. 3A). Some of the spores treated with  
260 200 mg L<sup>-1</sup>  $\epsilon$ -PL developed germ tubes (Fig. 3B), while others failed to germinate. The  
261 surface of the germ tubes appeared rough and irregular, and in some cases, it appeared as if  
262 the cellular contents had leaked out. At 400 mg L<sup>-1</sup> (Fig. 3C), only a few spores germinated  
263 normally, and most of them lost their morphological integrity. The damaged germ tubes  
264 appeared irregular with coarse surfaces. Cellular contents had leaked out and formed  
265 aggregates that adhered to the shriveled germ tubes. All of the conidia treated with 600 mg  
266 L<sup>-1</sup>  $\epsilon$ -PL failed to germinate and the spores appeared degraded, making them hard to  
267 recognize (Fig. 3D). Leaked cellular materials also appeared as aggregates that adhered to the  
268 degraded spores. These results indicated that the level of spore degradation increased with  
269 increasing concentrations of  $\epsilon$ -PL.

### 270 3.4. Intracellular ROS and loss of cell membrane integrity

271 Fig. 4A ROS production in *P. expansum* spores treated with  $\epsilon$ -PL was monitored using  
272 DCFH-DA staining. The intensity of the green fluorescence of conidia treated with 400 mg  
273 L<sup>-1</sup>  $\epsilon$ -PL was stronger than it was in conidia treated with 200 mg L<sup>-1</sup>  $\epsilon$ -PL. The percentage of  
274 conidia exhibiting green fluorescence in the 200 mg L<sup>-1</sup> and 400 mg L<sup>-1</sup>  $\epsilon$ -PL treatment  
275 groups was 15.42 % and 71.37 %, respectively (Fig. 4C). These results indicate that the

276 number of spores producing ROS increased as the concentration of  $\epsilon$ -PL increased.  $\epsilon$ -PL also  
277 disrupted the integrity of the plasma membrane in spores of *P. expansum*, as determined using  
278 PI staining (Fig. 4B). When the concentration of  $\epsilon$ -PL was increased from 200 to 400 mg L<sup>-1</sup>,  
279 the corresponding red fluorescence intensity was significantly enhanced (Fig. 4B), and the  
280 percentage of conidia that appeared to lose membrane integrity also increased from 10.28 %  
281 to 52.36 % (Fig. 4D).

### 282 3.5. Effect of $\epsilon$ -PL on the loss of cellular contents in vitro

283 The leakage of cellular soluble proteins (Fig. 5A) and nucleic acids (Fig. 5B) from the  
284 mycelia of *P. expansum* into the culture medium increased dramatically, relative to the control,  
285 when the concentration of  $\epsilon$ -PL was increased from 200 mg L<sup>-1</sup> to 400 mg L<sup>-1</sup>. The mycelia of  
286 *P. expansum* began to release soluble proteins and nucleic acids after one hour of exposure to  
287  $\epsilon$ -PL. The level of leakage of soluble proteins and nucleic acids into the culture medium  
288 reached its highest level, after 4 h, indicating that most of the mycelia had been disrupted by  
289 this time. The amount of materials leaked into the culture medium was positively correlated  
290 with the concentration of  $\epsilon$ -PL. These results indicate that  $\epsilon$ -PL damaged the integrity of the  
291 plasma membrane of *P. expansum* mycelia resulting in the loss of cellular contents into the  
292 culture medium.

### 293 3.6. Defense-related enzyme activity and corresponding defense-related gene expression in 294 apples

#### 295 3.6.1. Effect of $\epsilon$ -PL on defense-related enzyme activity in apple fruit

296 The pattern of PAL activity in treated and untreated apple tissue is presented in Fig. 6A.  
297 While the overall pattern was similar in both  $\epsilon$ -PL-treated and control apple tissues, distinct

298 differences were also evident. Over the course of seven days after being treated with  $\epsilon$ -PL,  
299 PAL enzyme activity first rose and then fell, and then subsequently rose and fell once more.  
300 PAL enzyme activity in the treatment group was similar to the control group on day 3 but  
301 otherwise significantly higher than the control group on the other days. PAL activity reached  
302 its maximum on day 4 in both treatment and control groups of apples.

303 The pattern of PPO activity in both  $\epsilon$ -PL-treated and control apple tissues was similar to  
304 the results obtained for PAL (Fig. 6B). PPO activity increased to a maximum peak after 4 d.  
305 PPO activity was always higher in  $\epsilon$ -PL-treated apple tissues than in non-treated, control  
306 apple tissues. As indicated in Fig. 6C and 6D, the pattern of CAT and POD activity in  
307  $\epsilon$ -PL-treated and control apple tissues apples was also similar to the results obtained for PAL  
308 and PPO. CAT and POD exhibited their highest activity in both groups on day 4 and 5,  
309 respectively. Notably, the level of CAT and POD activity was always higher in  $\epsilon$ -PL-treated  
310 apple tissues than it was in the non-treated tissues. These studies suggest that wounding  
311 induces defense-related enzyme activity but that treatment of wounds with  $600 \text{ mg L}^{-1}$   $\epsilon$ -PL  
312 induces a higher level of enzyme activity, which presumably contributed to the inhibition of  
313 blue mold (*P. expansum*).

### 314 3.6.2. Effect of $\epsilon$ -PL on defense-related enzyme gene expression in apple fruit

315 The expression level of the genes encoding the defense-related enzymes that were  
316 measured were also assessed in the same samples by RT-qPCR. From, *PAL* expression in  
317 apples began to rise one day after being treated with  $\epsilon$ -PL, and reached a peak of expression  
318 at 4 and 5 days (Fig. 7A). *PAL* expression was about 4.3 times higher in than the control in  
319  $\epsilon$ -PL-treated apple tissues on the fifth day after treatment.  $\epsilon$ -PL treatment also induced the

320 up-regulation of both *PPO* and *CAT* beginning on day 1, all the way through day 7 (Fig. 7B  
321 and Fig. 7C, respectively). The maximum level of *PPO* expression in  $\epsilon$ -PL-treated apple  
322 tissues was observed on the 2<sup>nd</sup> and 5<sup>th</sup> day after treatment, at which time it was 5.45 times  
323 higher than in the control. *CAT* expression in  $\epsilon$ -PL-treated apple tissues reached its highest  
324 value on the 4<sup>th</sup> day after treatment, at which time it was 4.05 times higher than it was in the  
325 control. *POD* expression in  $\epsilon$ -PL-treated apple tissues was up-regulated on the first, fifth,  
326 sixth, and seventh day after treatment (Fig. 7D). The highest level of *POD* expression in  
327  $\epsilon$ -PL-treated apple tissues occurred on the first day, at which time it was 3.44 times higher  
328 than the control (Fig. 7D). In general, the expression level of the measured defense-related  
329 enzyme genes was significantly up-regulated in apple tissues by treatment of wounds with  
330 600 mg L<sup>-1</sup>  $\epsilon$ -PL. These results were in general agreement with the measured levels of activity  
331 of the corresponding enzymes.

#### 332 **4. Discussion**

333  $\epsilon$ -PL is a safe, non-toxic natural food preservative that is widely used to control  
334 foodborne pathogenic bacterial contamination in baked goods, cooked meat products, fruit  
335 and vegetable beverages, and noodle products. Despite its antimicrobial properties, it has  
336 been rarely tested for its ability to inhibit fungal contamination of food products or  
337 postharvest diseases of fruit. Previous studies have been conducted on the inhibitory effect of  
338  $\epsilon$ -PL on citrus fruit disease caused by *Penicillium digitatum* and jujube fruit disease caused by  
339 *Botrytis cinerea*, however, the ability of  $\epsilon$ -PL to induce disease resistance in fruit has not been  
340 fully investigated in these studies (Liu et al., 2017; Li et al., 2019). More specifically, studies  
341 on the inhibitory effect of  $\epsilon$ -PL on blue mold disease in apples or its potential effect on the

342 induction of disease resistance has not been conducted. The present study is the first report on  
343 the use of  $\epsilon$ -PL to inhibit postharvest decay in apple fruit caused by *P. expansum*. Results of  
344 our study revealed that  $\epsilon$ -PL significantly inhibited conidial germination in *P. expansum* and  
345 mycelial growth *in vitro* and *in vivo*. Furthermore, the study provided evidence of the ability  
346 of  $\epsilon$ -PL to induce a resistance response in apples.

347  $\epsilon$ -PL in a concentration range of 400 mg L<sup>-1</sup> and 600 mg L<sup>-1</sup> provided effective  
348 protection against blue mold decay in apples. Concentrations above or below this range were  
349 comparatively less efficient in inhibiting blue mold decay. Compared to the antifungal  
350 activity *in vitro*, a higher concentration of  $\epsilon$ -PL was needed to effectively inhibit germination  
351 and mycelial growth in treated apples than was needed to achieve the same effect under *in*  
352 *vitro* culture conditions. There are three possible reasons to explain these results. Firstly,  $\epsilon$ -PL  
353 may be absorbed into the apple tissue after it is administered, thereby reducing the amount of  
354  $\epsilon$ -PL to which the fungus is exposed. Secondly,  $\epsilon$ -PL entering the apple tissue may react with  
355 the apple tissue matrix, changing the molecular structure of the  $\epsilon$ -PL, thus reducing its  
356 antimicrobial properties. Thirdly, a low concentration of  $\epsilon$ -PL may not be sufficient to  
357 activate a resistance response in apple tissues, while too high a concentration may be  
358 cytotoxic to apple cells which may die or leak nutrients making them available for fungal  
359 growth. Notably, our study indicated that the optimal concentration of  $\epsilon$ -PL needed to inhibit  
360 blue mold decay in apples was significantly lower than the concentration needed to inhibit *P.*  
361 *digitatum* in citrus fruit and *B. cinerea* in jujube fruit. This would make the application of  
362  $\epsilon$ -PL in apples more economic and also reduce potential residues.

363 DCFH-DA and PI staining methods were used to detect the level of ROS production and  
364 quantify the level of damaged cells, respectively. The DCFH-DA results revealed that high  
365 levels of ROS were produced and the results with PI revealed that that the number of  
366 damaged *P. expansum* spores was very high when they were exposed to 600 mg L<sup>-1</sup> ε-PL.  
367 Excessive ROS production results in oxidative injury to mitochondria and cell components  
368 such as proteins and lipids. This damage results in cell dysfunction and the suppression of  
369 spore germination, mycelial growth, all of which reduce pathogenicity. SEM observations  
370 revealed that the leakage of cell contents from spores was positively proportional to the  
371 concentration of ε-PL. This suggests that the higher concentrations of ε-PL degrade the cell  
372 walls of spores and cause a loss of membrane integrity, in some cases killing the spores of *P.*  
373 *expansum*.

374 PAL, PPO, CAT, and POD are four important defense-related enzymes that contribute to  
375 innate disease resistance in fruits. The level of activity of these enzymes are positively  
376 correlated with fruit disease resistance, and thus, they can be used as indicators of the level of  
377 fruit disease resistance (Qin et al., 2015; Zhang et al., 2016). Phenolic compounds, flavonoids,  
378 and lignin are primary antifungal compounds which are synthesized in the phenylpropanoid  
379 pathway. PPO has a vital function in host plant defense mechanisms, participates in the  
380 metabolism of phenols, converts phenolic compounds to more toxic quinone, and so its  
381 activity would enhance disease resistance in apple fruit tissues. PAL is a crucial rate-limiting  
382 enzyme in the shikimic acid pathway that plays a primary role in the production of secondary  
383 metabolites, including phenolic compounds, and lignin. POD and CAT are antioxidant  
384 enzymes that help prevent excessive ROS accumulation in plant cells. In that the present

385 study, PAL, PPO, CAT, and POD activity significantly increased in apple tissues treated with  
386 600 mg L<sup>-1</sup> ε-PL for 24 h, indicating that ε-PL induced a defense response in apple tissues.  
387 The expression level of genes encoding the four defense enzymes were assessed by RT-qPCR,  
388 and further confirmed that 600 mg L<sup>-1</sup> ε-PL of activates a defense response in apple tissues.  
389 Our results demonstrated that ε-PL induced apples to up-regulate the expression of *PPO*, *CAT*,  
390 *POD*, and *PAL* genes, which resulted increased activity of the four corresponding  
391 defense-related enzymes, leading to enhanced resistance to blue mold decay in apple fruit.  
392 Overall, the increased activity of defense-related enzymes may have contributed to enhanced  
393 resistance by increasing the synthesis of antifungal compounds and managing oxidative stress  
394 in apple cells. Future experiments will further explore the molecular mechanism underlying  
395 the ε-PL-induced enhanced resistance of apple to blue mold decay, and include both  
396 transcriptomic and proteomic analyses.

## 397 **5. Conclusions**

398 Results of the present study demonstrated that ε-PL effectively inhibits postharvest blue  
399 mold decay in apples. The optimal concentration of ε-PL in apples was 600 mg L<sup>-1</sup>.  
400 Concentration of ε-PL above 200 mg L<sup>-1</sup> had an inhibitory effect on *P. expansum in vitro*,  
401 with the level of inhibition being concentration dependent. The study also suggested three  
402 possible mechanisms associated with ε-PL inhibition of *P. expansum*. Firstly, ε-PL has the  
403 ability to induce the up-regulation of defense-related gene expression and increase  
404 corresponding defense-related enzyme activity of PAL, PPO, CAT, and POD in apples tissues.  
405 Secondly, exposure of *P. expansum* to ε-PL resulted in excessive intracellular ROS  
406 production in spores, which may have injured or killed spores, thus reducing or eliminating

407 spore germination or mycelial growth. Thirdly,  $\epsilon$ -PL may degrade the cell wall and reduce the  
408 integrity of the plasma membrane of *P. expansum* conidia, causing a large amount of cellular  
409 materials to leak out of the cells, again reducing or eliminating spore germination and  
410 mycelial growth. Further molecular studies will be required, however, to firmly establish the  
411 mechanisms by which  $\epsilon$ -PL limits spore germination and mycelial growth of *P. expansum*,  
412 and enhances disease resistance in apple tissues.

### 413 **Conflict of interest**

414 The authors declare that there is no conflicts of interest.

### 415 **Acknowledgements**

416 This work was supported by the National Natural Science Foundation of China  
417 (31772037; 31901743).

418 We thank Dr. Michael Wisniewski from Virginia Polytechnic Institute and State  
419 University, Blacksburg, VA, USA, for his critical reading of the manuscript.

### 420 **References**

- 421 Apaliya, M.T., Zhang, H., Yang, Q., Zheng, X., Zhao, L., Kwaw, E., Mahunu, G.K., 2017.  
422 *Hanseniaspora uvarum* enhanced with trehalose induced defense-related enzyme  
423 activities and relative genes expression levels against *Aspergillus tubingensis* in table  
424 grapes. Postharvest Biol. Technol. 132, 162–170.  
425 <https://doi.org/10.1016/j.postharvbio.2017.06.008>
- 426 Bhattacharya, S., Bhayani, K., Ghosh, T., Bajaj, S., Trivedi, N., et al., 2018. Stability of  
427 phycobiliproteins using natural preservative  $\epsilon$ -Polylysine ( $\epsilon$ -PL). Ferment Technol. 7,  
428 149.

429 <https://doi.org/10.4172/2167-7972.1000149>

430 Bradford, M.M., 1976. A rapid and sensitive method for the quantitation of microgram  
431 quantities of protein utilizing the principle of protein–dye binding. *Anal. Biochem.* 72,  
432 248–254.

433 [https://doi.org/10.1016/0003-2697\(76\)90527-3](https://doi.org/10.1016/0003-2697(76)90527-3)

434 Cai, J.H, Chen,J., Lu, G.B., Zhao, Y.M., Tian, S.P., Qin, G.Z., 2015. Control of brown rot on  
435 jujube and peach fruits by trisodium phosphate. *Postharvest Biol. Technol.* 99, 93-98.

436 <https://doi.org/10.1016/j.postharvbio.2014.08.003>

437 Cui, H.Y., Zhang, C.H., Li, C.Z., Lin, L., 2018. Antimicrobial mechanism of clove oil on  
438 *Listeria monocytogenes*. *Food Control.* 94, 140-146.

439 <https://doi.org/10.1016/j.foodcont.2018.07.007>

440 Daniel, C.K., et al., 2015. *In vivo* application of garlic extracts in combination with clove oil  
441 to prevent postharvest decay caused by *Botrytis cinerea*, *Penicillium expansum* and  
442 *Neofabraea alba* on apples. *Postharvest Biol. Technol.* 99, 88-92.

443 <https://doi.org/10.1016/j.postharvbio.2014.08.006>

444 Errampalli, D., 2014. *Penicillium expansum* (Blue Mold) Postharvest Decay Control, in:  
445 Bautista-Baños, S., *Strategies Academic Press*, 189-231.

446 <https://doi.org/10.1016/B978-0-12-411552-1.00006-5>

447 Förster, H., Driever, G.F., Thompson, D.C., Adaskaveg, J.E., 2007. Postharvest decay  
448 management for stone fruit crops in California using the “reduced-risk” fungicides  
449 fludioxonil and fenhexamid. *Plant Dis.* 91, 209–215.

450 <https://doi.org/10.1094/pdis-91-2-0209>

451 Ge, Y. H., Wei, M. L., Li, C. Y., Chen, Y. R., Lv, J. Y., Meng, K., Wang, W. H., Li, J. R., 2018.  
452 Reactive oxygen species metabolism and phenylpropanoid pathway involved in disease  
453 resistance against *Penicillium expansum* in apple fruit induced by  $\epsilon$ -poly-L-lysine. J. Sci.  
454 Food Agric. 98, 5082-5088.  
455 <https://doi.org/10.1002/jsfa.9046>

456 He, L.L., Liu, Y., Mustapha, A., Lin, M.S., 2011. Antifungal activity of zinc oxide  
457 nanoparticles against *Botrytis cinerea* and *Penicillium expansum*. Microbiol. Res. 166,  
458 207-215.  
459 <https://doi.org/10.1016/j.micres.2010.03.003>

460 Hosomi, R., Yamamoto, D., Otsuka, R., Nishiyama, T., Yoshida, M., Fukunaga, K., 2015.  
461 Dietary varepsilon-polylysine decreased serum and liver lipid contents by enhancing  
462 fecal lipid excretion irrespective of increased hepatic fatty acid biosynthesis-related  
463 enzymes activities in rats. Prev. Nutr. Food Sci. 20, 43-51.  
464 <https://doi.org/10.3746/pnf.2015.20.1.43>

465 Hyldgaard, M., Mygind, T., Vad, B.S., Stenvang, M., Otzen, D.E., Meyer, R.L., 2014. The  
466 antimicrobial mechanism of action of epsilon-poly-L-lysine. Appl. Environ. Microbiol..  
467 80, 7758–7770.  
468 <https://doi.org/10.1128/aem.02204-14>

469 Li, H., He, C., Li, G. J., Zhang, Z. Q., Li, B. Q., Tian, S. P., 2019. The modes of action of  
470 epsilon-polylysine ( $\epsilon$ -PL) against *Botrytis cinerea* in jujube fruit. Postharvest Biol.  
471 Technol. 147, 1-9.  
472 <https://doi.org/10.1016/j.postharvbio.2018.08.009>

473 Li, J.K., Lei, H. H., Song, H. M., Lai, T. F., Xu, X. B., Shi, X.Q., 2017a.  
474 1-methylcyclopropene (1-MCP) suppressed postharvest blue mold of apple fruit by  
475 inhibiting the growth of *Penicillium expansum*. Postharvest Biol. Technol. 125, 59-64.  
476 <https://doi.org/10.1016/j.postharvbio.2016.11.005>

477 Li, S.F., Zhang, L. H., Liu, M. P., Wang, X. Y., Zhao, G. Y., Zong, W, 2017b. Effect of  
478 poly-ε-lysine incorporated into alginate-based edible coatings on microbial and  
479 physicochemical properties of fresh-cut kiwi-fruit. Postharvest Biol. Technol. 134,  
480 114–121.  
481 <https://doi.org/10.1016/j.postharvbio.2017.08.014>

482 Li, Y.Q., Feng, J.L., Han, Q., Dai, Z.Y., Liu, W., Mo, H.Z., 2014a. Effects of e-polylysine on  
483 physicochemical characteristics of chilled pork. Food Bioprocess Technol. 17,  
484 2507–2515.  
485 <https://doi.org/10.1007/s11947-013-1223-4>

486 Li, Y.Q., Han, Q., Feng, J.L., Tian, W.L., Mo, H.Z., 2014b. Antibacterial characteristics and  
487 mechanisms of e-poly-lysine against *Escherichia coli* and *Staphylococcus aureus*. Food  
488 Control. 43, 22–27.  
489 <https://doi.org/10.1016/j.foodcont.2014.02.023>

490 Liu, K.W., Zhou X.J., Fu, M.R., 2017. Inhibiting effects of epsilon-poly-lysine (ε-PL) on  
491 *Pencillium digitatum* and its involved mechanism. Postharvest Biol. Technol. 123,  
492 94-101.  
493 <https://doi.org/10.1016/j.postharvbio.2016.08.015>

494 Livak, K.J., Schmittgen, T.D., 2001. Analysis of relative gene expression data using real-time

495 quantitative PCR and the  $2^{-\Delta\Delta CT}$  method. *Methods*. 25, 402-408.

496 <https://doi.org/10.1006/meth.2001.1262>

497 Mahunu, G.K., Zhang, H. Y., Apaliya, M.T., Yang, Q. Y., Zhang, X. Y., Zhao, L. N., 2018.

498 Bamboo leaf flavonoid enhances the control effect of *Pichia caribbica* against

499 *Penicillium expansum* growth and patulin accumulation in apples. *Postharvest Biol.*

500 *Technol.* 141, 1-7.

501 <https://doi.org/10.1016/j.postharvbio.2018.03.005>

502 Pandey, A. K., Kumar, A., 2014. Improved microbial biosynthesis strategies and multifarious

503 applications of the natural biopolymer epsilon-poly-l-lysine. *Process Biochem.* 49,

504 496–505.

505 <https://doi.org/10.1016/j.procbio.2013.12.009>

506 Pietrysiak, E., Ganjyal,G.M., 2018. Apple peel morphology and attachment of *Listeria*

507 *innocua* through aqueous environment as shown by scanning electron microscopy. *Food*

508 *Control.* 92,362-369.

509 <https://doi.org/10.1016/j.foodcont.2018.04.049>

510 Qin, X., Xiao, H., Xue, C., Yu, Z., Yang, R., Cai, Z., Si, L., 2015. Biocontrol of Gray Mold in

511 Grapes with the Yeast *Hanseniaspora uvarum* alone and in Combination with Salicylic

512 Acid or Sodium Bicarbonate. *Postharvest Biol. Technol.* 100, 160-167.

513 <https://doi.org/10.1016/j.postharvbio.2014.09.010>

514 Salomao, B.C., Aragao, G.M., Churey, J.J., Worobo, R.W., 2008. Efficacy of sanitizing

515 treatments against *Penicillium expansum* inoculated on six varieties of apples. *J. Food*

516 *Prot.* 71, 643–647.

517 <https://doi.org/10.4315/0362-028X-71.3.643>

518 Sansone, G., Rezza, I., Calvente, V., Benuzzi, D., Tosetti, M.I., 2005. Control of *Botrytis*  
519 *cinerea* strains resistant to iprodione in apple with rhodotorulic acid and yeasts.  
520 Postharvest Biol. Technol. 35, 245-251.  
521 <https://doi.org/10.1016/j.postharvbio.2004.09.005>

522 Sharma, R.R., Singh, D., Singh, R., 2009. Biological control of postharvest diseases of fruits  
523 and vegetables by microbial antagonists: a review. Biol. Control. 50, 205–221.  
524 <https://doi.org/10.1016/j.biocontrol.2009.05.001>

525 Shi, X. Q., Li, B. Q., Qin, G. Z., Tian, S. P., 2012. Mechanism of antifungal action of borate  
526 against *Colletotrichum gloeosporioides* related to mitochondrial degradation in spores.  
527 Postharvest Biol. Technol. 67, 138–143.  
528 <https://doi.org/10.1016/j.postharvbio.2012.01.003>

529 Shima, S., Sakai, H., 1977. Polylysine produced by streptomyces. Agric. Biol. Chem. 41,  
530 1807–1809.  
531 <https://doi.org/10.1080/00021369.1977.10862764>

532 Su, R.H., Li, T.F., Fan, D., Huang, J.L., Zhao, J.X., Yan, B.W., Zhou, W.G., Zhang, W.H.,  
533 Zhang, H., 2018. The inhibition mechanism of  $\epsilon$ -Polylysine against *Bacillus cereus*  
534 emerging in surimi gel during refrigerated storage. J. Sci. Food Agric. 99, 2922-2930.  
535 <https://doi.org/10.1016/j.postharvbio.2016.11.005>

536 Sun, G.Z., Yang, Q.C., Zhang, A.C., Guo, J., Liu, X.L., Wang, Y., Ma, Q., 2018. Synergistic  
537 effect of the combined bio-fungicides  $\epsilon$ -poly-l-lysine and chitooligosaccharide in

538 controlling grey mould (*Botrytis cinerea*) in tomatoes. Int. J. Food Microbiol. 276,  
539 46–53.  
540 <https://doi.org/10.1016/j.ijfoodmicro.2018.04.006>

541 Tuersuntuoheti T, Wang, Z.H., Wang, Z.Y., Liang, S., Li, X.P., Zhang, M., 2019. Review of  
542 the application of  $\epsilon$ -poly-L-lysine in improving food quality and preservation. J Food  
543 Process Preserv. 43, e14153.  
544 <https://doi.org/10.1111/jfpp.14153>

545 Wang, M.Y., Zhao, L.N., Zhang, X.Y., Dhanasekaran, S., Abdelhai, M.H., Yang, Q.Y., Jiang,  
546 Z.H., Zhang, H.Y., 2019. Study on biocontrol of postharvest decay of table grapes  
547 caused by *Penicillium rubens* and the possible resistance mechanisms by *Yarrowia*  
548 *lipolytica*. Biol. Control. 130, 110-117.  
549 <https://doi.org/10.1016/j.biocontrol.2018.11.004>

550 Wang, Y., Li, Y.L., Xu, W.D., Zheng, X.F., Zhang, X.Y., Abdelhai, M.H., Zhao, L.N., Li, H.F.,  
551 Diao, J.W., Zhang, H.Y., 2018. Exploring the effect of  $\beta$ -glucan on the biocontrol  
552 activity of *Cryptococcus podzolicus* against postharvest decay of apples and the possible  
553 mechanisms involved. Biol. Control 121, 14–22.  
554 <https://doi.org/10.1016/j.biocontrol.2018.02.001>

555 Ye, R.S., Xu, H.Y., Wan, C.X., Peng, S.S., Wang, L.J., Xu, H., Aguilar, Z.P., Xiong, Y. H.,  
556 Zeng, Z.L., Wei, H., 2013. Antibacterial activity and mechanism of action of  
557  $\epsilon$ -poly-l-lysine. Biochem. Biophys. Res. Commun. 439, 148–153.  
558 <https://doi.org/10.1016/j.bbrc.2013.08.001>

559 Zhang, L.M., Li, R.C., Dong, F., Tian, A.Y., Li, Z.J., Dai, Y. J., 2015. Physical, mechanical  
560 and antimicrobial properties of starch films incorporated with  $\epsilon$ -poly-L-lysine. Food  
561 Chem. 166, 107–114.  
562 <https://doi.org/10.1016/j.foodchem.2014.06.008>

563 Zhang, X., Li, Y., Wang, H., Gu, X., Zheng, X., Wang, Y., Diao, J., Peng, Y., Zhang, H., 2016.  
564 Screening and identification of novel ochratoxin a-producing fungi from grapes. Toxins  
565 (Basel). 8, 333.  
566 <https://doi.org/10.3390/toxins8110333>

567 Zhang, X.W., Shi,C., Liu, Z.J., Pan F.G., Meng, R.Z., Bu, X.J., Xing, H.Q., Deng, Y.H. Guo,  
568 N., Yu,L., 2018. Antibacterial activity and mode of action of  $\epsilon$ -polylysine against  
569 *Escherichia coli* O157:H7. J. Med. Microbiol..67, 838–845.  
570 <https://doi.org/10.1099/jmm.0.000729>

571 Zhang, X.Y., Zhang, G.C., Li, P.X., Yang, Q.Y., Chen, K.P., Zhao, L.N., Apaliya, M. T., Gu,  
572 X., Zhang, H.Y., 2017. Mechanisms of glycine betaine enhancing oxidative stress  
573 tolerance and biocontrol efficacy of *Pichia caribbica* against blue mold on apples. Biol.  
574 Control. 108, 55-63.  
575 <https://doi.org/10.1016/j.biocontrol.2017.02.011>

576 Zhao, L., Wang, Y., Wang, Y., Li, B., Gu, X., Zhang, X., Boateng, N.A.S., Zhang, H., 2020.  
577 Effect of  $\beta$ -glucan on the biocontrol efficacy of *Cryptococcus podzolicus* against  
578 postharvest decay of pears and the possible mechanisms involved. Postharvest Biol.  
579 Technol. 160, 111057.  
580 <https://doi.org/10.1016/j.postharvbio.2019.111057>

581 Zheng, X. F., Yang, Q. Y., Zhang, X. Y., Apaliya, M.T., Ianiri, G., Zhang, H. Y., Castoria, R.,  
582 2017. Biocontrol agents increase the specific rate of patulin production by *Penicillium*  
583 *expansum* but decrease the disease and total patulin contamination of apples. Front.  
584 Microbiol. 8.  
585 <https://doi.org/10.3389/fmicb.2017.01240>

586 Zhu, Y.L., Li, C.Z., Cui, H.Y., Lin, L., 2019. Antimicrobial mechanism of pulsed light for the  
587 control of *Escherichia coli* O157:H7 and its application in carrot juice. Food Control.  
588 106.  
589 <https://doi.org/10.1016/j.foodcont.2019.106751>

590  
591

592

593 **Table. 1** Primers used in RT-qPCR reactions of defense-related relative gene expressions in

594 apples.

Gene name	Accession number	Primer	Primer Sequence (5' → 3')
<i>Polyphenoloxidase (PPO)</i>	LOC103446446	F- <i>PPO</i> - qRT	ATGCCAAGTCCAAGAGCCAA
		R- <i>PPO</i> - qRT	CCAGTGCCGGATTGGTTGTA
<i>Peroxidase (POD)</i>	LOC103444817	F- <i>POD</i> - qRT	AAGCCTATAGCCCCACCAGA
		R- <i>POD</i> - qRT	CTTGAAGCTACGTGGGTCGT
<i>Catalase (CAT)</i>	LOC103445262	F- <i>CAT</i> - qRT	AGACACCTGTCATTGTGCGT
		R- <i>CAT</i> - qRT	ACACGAGGGTTCGGATAGGG
<i>Phenylalanine ammonia lyase (PAL)</i>	LOC103419282	F- <i>PAL</i> - qRT	GGCATTGAGGAGAACTTG
		R- <i>PAL</i> - qRT	AGAACCTTGAGGGGTGAAGC
<i>ACTIN</i>	LOC103447714	F- <i>ACTIN</i> - qRT	CCCAAAGGCTAATCGGGAGAAA
		R- <i>ACTIN</i> - qRT	ACCACTGGCGTAGAGGGAAAGA

595

596 **Figure Caption**597 **Fig. 1.** The effect of different concentrations of  $\epsilon$ -PL on blue mold decay in apples caused by598 *Penicillium expansum*. Apples were treated with 30  $\mu$ L of 0, 100, 200, 400, 600, or 800 mg599  $L^{-1}$   $\epsilon$ -PL for 24 h at 20°C, 95% RH. Subsequently, 30  $\mu$ L of a *P. expansum* spore suspension600 ( $1 \times 10^5$  spores  $mL^{-1}$ ) was administered into each wound. Fruit were then stored for 6 d.

601 Representative photos were taken after 6 days (A), and decay incidence (B) and lesion

602 diameter (C) were assessed on days 3, 4, 5, and 6. Each treatment consisted of three replicates

603 and each replicate contained six apples and four wounds per apple, the experiment was

604 repeated twice. Data presented represent the mean  $\pm$  standard error,  $n = 3$ . Different small

605 letters over the columns indicate significant differences between treatments on the day of

606 assessment as determined by a Duncan's multiple range test ( $P < 0.05$ ).

607

608 **Fig. 2.** Scanning electron microscopy (SEM) images of the effect of  $\epsilon$ -PL on germination of *P.*  
609 *expansum* conidia in apples.  $\epsilon$ -PL (30  $\mu$ L) at 600 mg L<sup>-1</sup> and sterilized saline solution (30  $\mu$ L)  
610 as a control was added into the wounds made in apples. Apples were stored at 20 °C and  
611 95 % RH for 24 h prior to administering 30  $\mu$ L of a spore suspension (1  $\times$  10<sup>5</sup> spores mL<sup>-1</sup>) of  
612 *P. expansum* into each wound, after which the apples were then placed under the same storage  
613 conditions. Samples of the wounded tissues were removed from the apple at 9 h, 12 h, and 18  
614 hand prepared for SEM. The scale bar represents 10  $\mu$ m. Each treatment consisted of three  
615 replicates and the experiments were repeated twice.

616

617 **Fig. 3.** Scanning electron microscopy (SEM) images of mycelia and conidia of *P. expansum*  
618 treated with (A) 0 mg L<sup>-1</sup> (B) 200 mg L<sup>-1</sup> (C) 400 mg L<sup>-1</sup> (D) 600 mg L<sup>-1</sup>  $\epsilon$ -PL *in vitro* for 9 h.  
619 *P. expansum* spore suspensions (1 $\times$ 10<sup>5</sup> spores mL<sup>-1</sup>) were cultured in PDB media amended  
620 with  $\epsilon$ -PL (0, 200, 400, or 600 mg L<sup>-1</sup>) at 25 °C on a rotary shaker set at 150 rpm. After 9 h,  
621 the cultures were centrifuged for 3 min at 8000  $\times$  g and prepared for SEM. The scale bar  
622 represents 1 $\mu$ m. Each treatment consisted of three replicates and the experiments were  
623 repeated twice.

624

625 **Fig. 4.** Effect of  $\epsilon$ -PL on reactive oxygen species (ROS) production and membrane integrity  
626 of *P. expansum* conidia *in vitro*. Conidia were incubated in different concentrations of  $\epsilon$ -PL (0,  
627 200, and 400 mg L<sup>-1</sup>) for 9 h and then stained with 10  $\mu$ M of 2',7'-dichlorodihydrofluorescein  
628 diacetate (DCFH-DA) or 10 mg L<sup>-1</sup> of propidium iodide (PI). ROS production in conidia is  
629 indicated by green fluorescence (A), while loss of membrane integrity is indicated by red

630 fluorescence (B). Percentage of conidia exhibiting high levels of ROS (C), and the percentage  
631 of conidia exhibiting a loss of membrane integrity (D). Three fields of view, each containing  
632 at least 100 conidia were randomly selected for photographing. Each treatment consisted of  
633 three replicates and the experiments were repeated twice. Scale bar represents 50  $\mu\text{m}$ . Data  
634 represent the mean  $\pm$  standard error of the mean,  $n = 3$ . Different small letters over columns  
635 indicate significant differences between treatments as determined by a Duncan's multiple  
636 range test ( $P < 0.05$ ).

637

638 **Fig. 5.** Effect of different concentrations of  $\epsilon$ -PL on the amount of soluble protein and nucleic  
639 acid leakage from *P. expansum* conidia treated with 0, 200, and 400  $\text{mg L}^{-1}$   $\epsilon$ -PL. The washed  
640 mycelia were resuspended in 100 mL of sterile distilled water containing  $\epsilon$ -PL and placed at  
641 25  $^{\circ}\text{C}$  on a rotary shaker set at 150 rpm. The leakage of soluble proteins (A) is expressed as  
642 milligrams per liter of solution, while leakage of nucleic acids (B) is expressed as absorbance  
643 value at 260 nm ( $A_{260\text{nm}}$ ). Treatments: CK (sterile distilled water), A ( $\epsilon$ -PL at 200  $\text{mg L}^{-1}$ ), B  
644 ( $\epsilon$ -PL at 400  $\text{mg L}^{-1}$ ). Each treatment contained three replicates, and the experiment was  
645 repeated twice. Data presented represent the mean  $\pm$  standard error of the mean,  $n = 3$ .  
646 Asterisk (\*) indicates significant differences between the control and treatment by a Duncan's  
647 multiple range test ( $P < 0.05$ ).

648

649 **Fig. 6.** Time course changes in defense-related enzyme activity in apples induced by  $\epsilon$ -PL.  
650 Each wound in apples were administered 30  $\mu\text{L}$  of  $\epsilon$ -PL, while 30  $\mu\text{L}$  of sterilized saline  
651 solution was used as a control. Apple tissue around wounds was collected at 0, 1, 2, 3, 4, 5, 6,

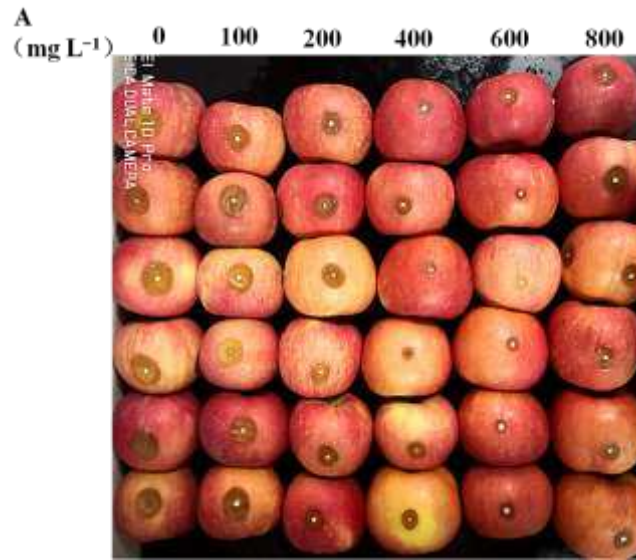
652 and 7 d after treatment and assayed for (A) PAL, (B) PPO, (C) CAT, and (D) POD activity.  
653 Treatments: CK - saline control, and  $\epsilon$ -PL at 600 mg L<sup>-1</sup>. Each treatment consisted of three  
654 replicates and the experiment was repeated twice. Data represent the mean  $\pm$  standard error ,  
655  $n = 3$ . Asterisk (\*) indicates significant differences between the control and treatment by a  
656 Duncan's multiple range test ( $P < 0.05$ ).

657

658 **Fig. 7.** Time course changes in defense-related enzyme gene expression in apples treated with  
659  $\epsilon$ -PL. Each wound in apples were administered 30  $\mu$ L of  $\epsilon$ -PL, while 30  $\mu$ L of sterilized  
660 saline solution was used as a control. Apple tissue around wounds was collected at 0, 1, 2, 3,  
661 4, 5, 6, and 7 d after treatment and the tissues were used to assess defense-related gene  
662 expression of (A) *PAL*, (B) *PPO*, (C) *CAT* and (D) *POD*. Treatments: CK - the saline control,  
663 and  $\epsilon$ -PL at 600 mg L<sup>-1</sup>. Each treatment consisted of three replicates and the experiment was  
664 repeated twice. Data represent the mean  $\pm$  standard error,  $n = 3$ . Different small letters above  
665 columns indicate significant differences between the level of expression in the apple tissues  
666 treated with  $\epsilon$ -PL as determined by a Duncan's multiple range test ( $P < 0.05$ ).

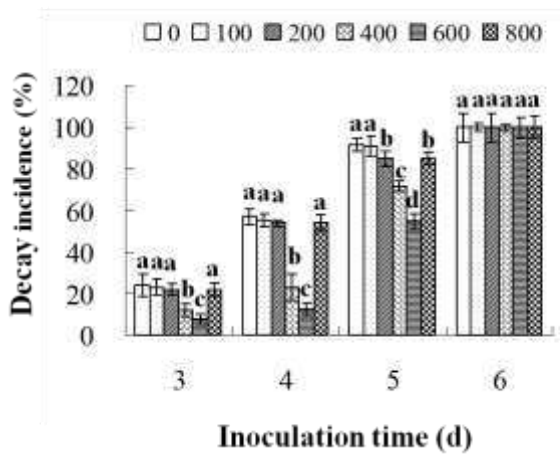
667

668 Fig.1

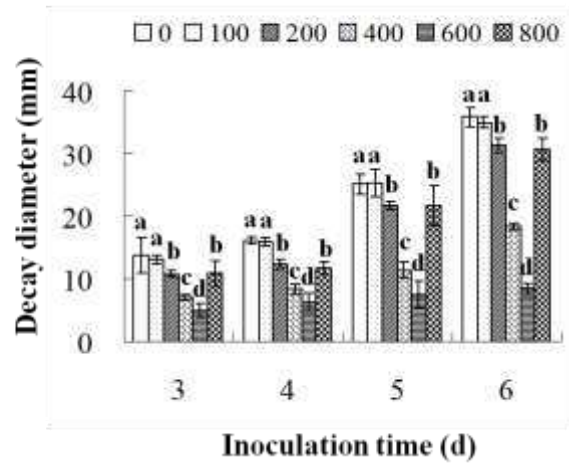


669

**B**



**C**

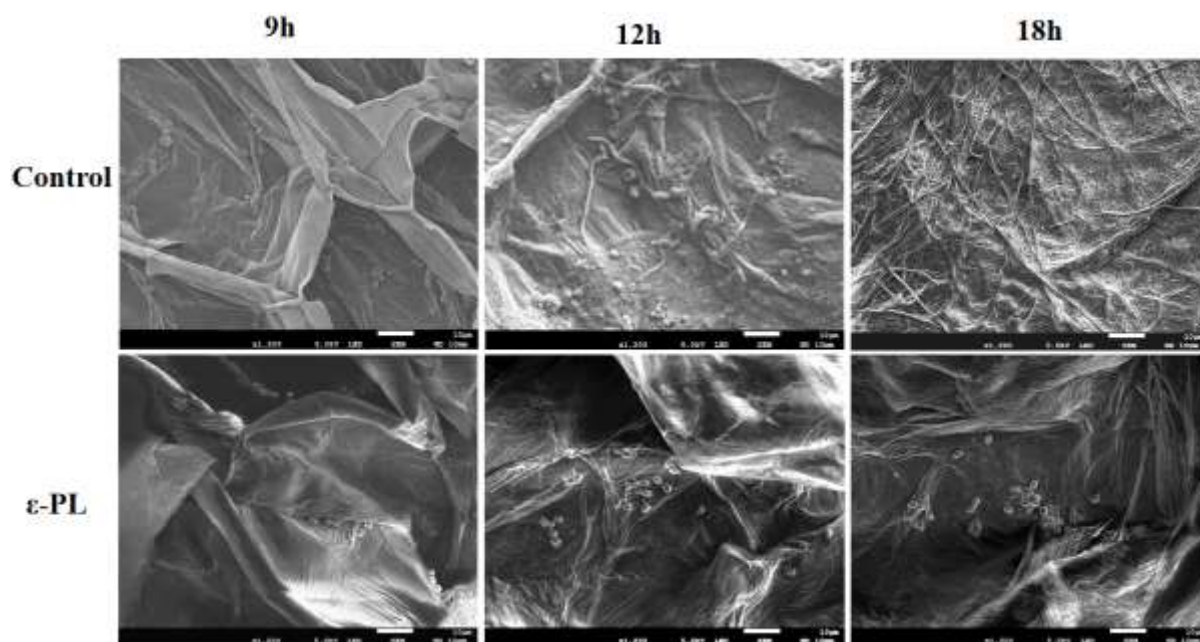


670

671

672

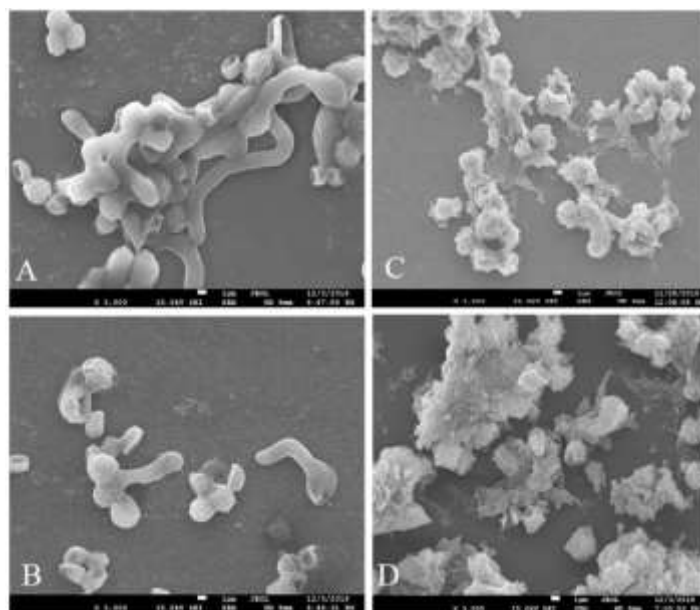
673 **Fig.2**



674

675

676 **Fig.3**

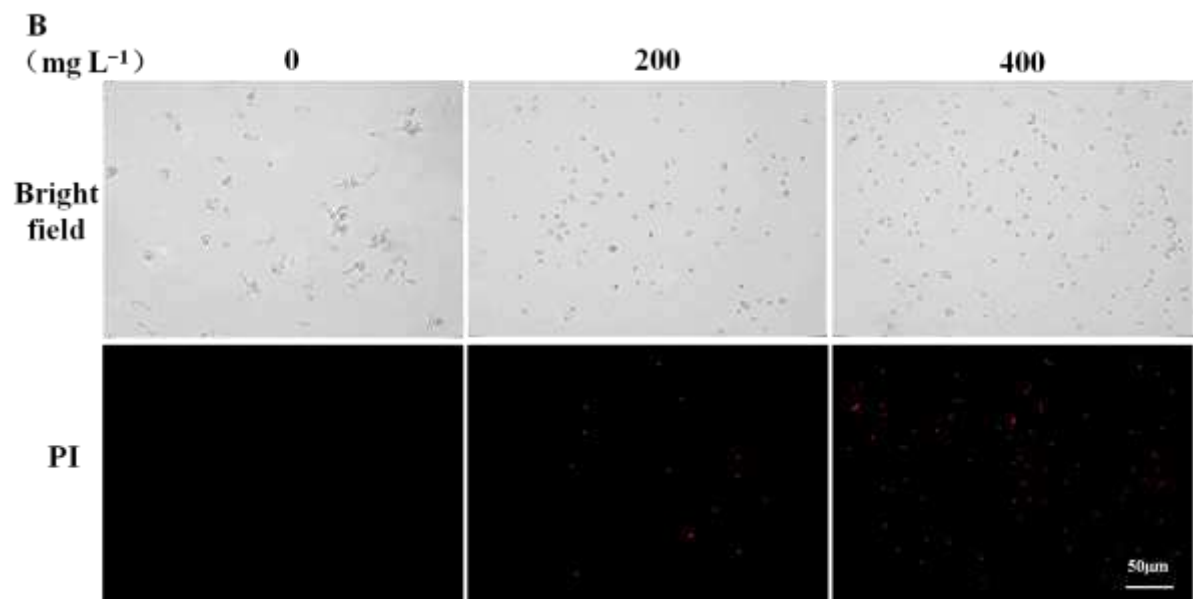
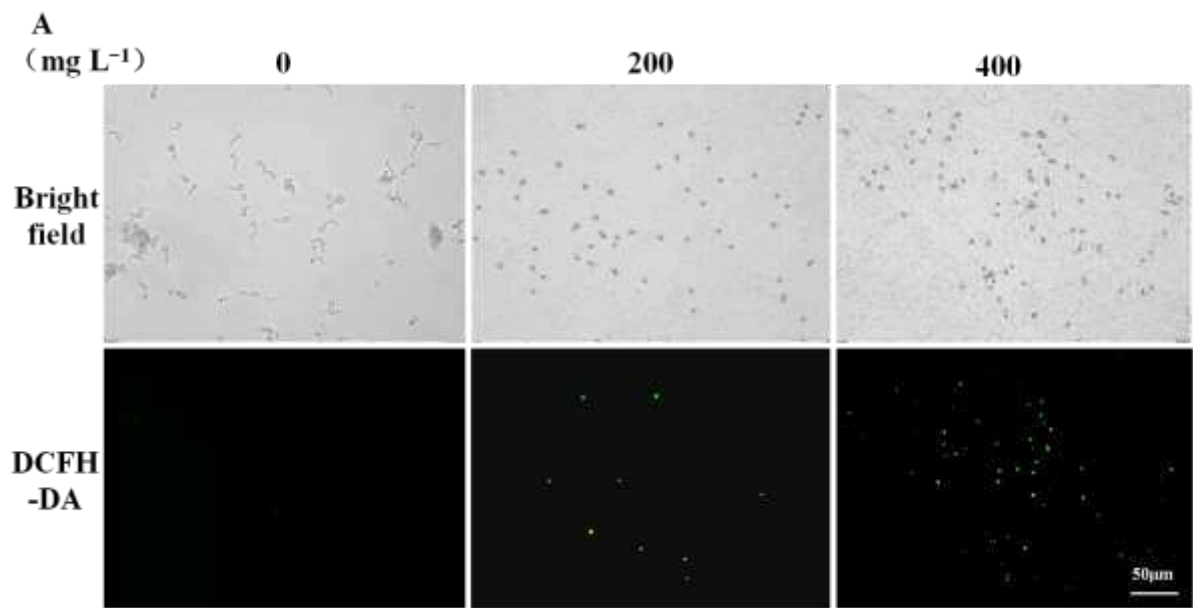


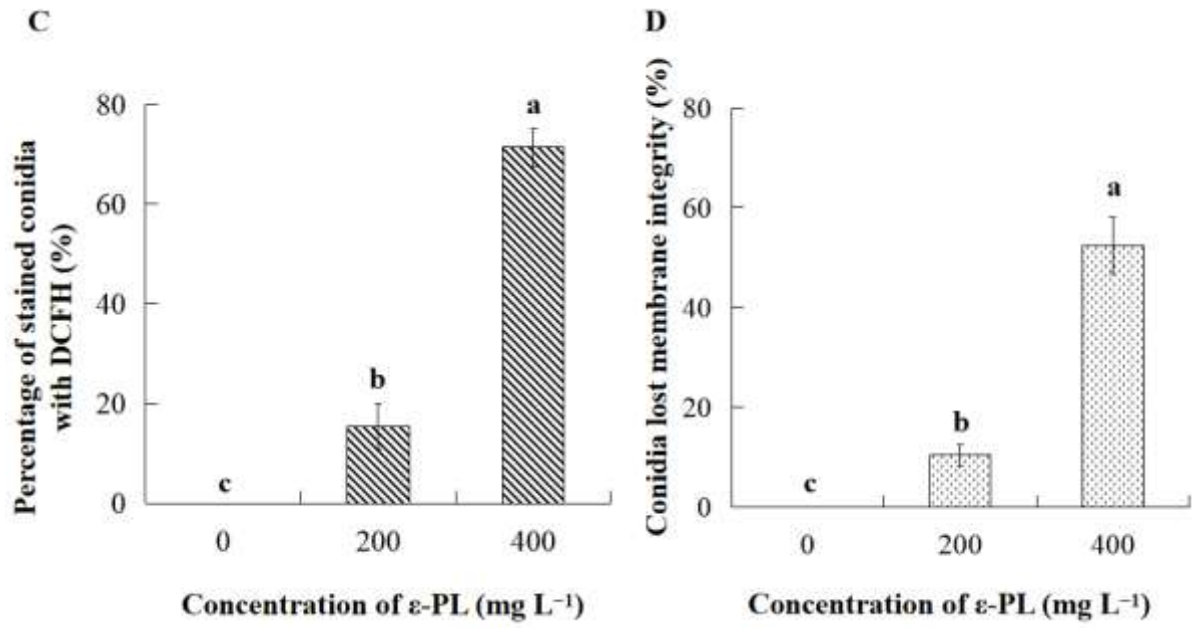
677

678

679

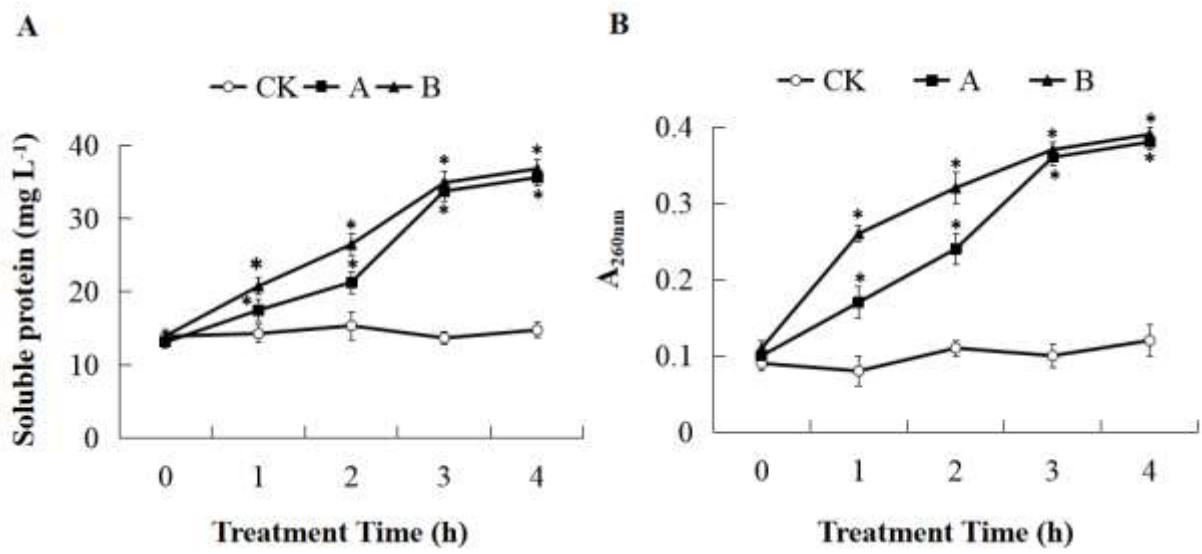
680 **Fig.4**





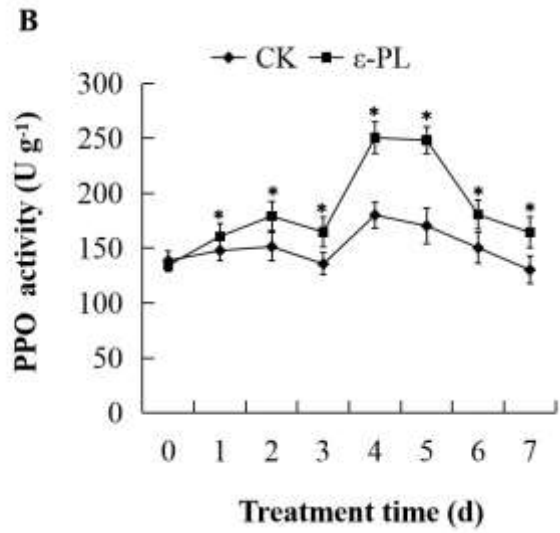
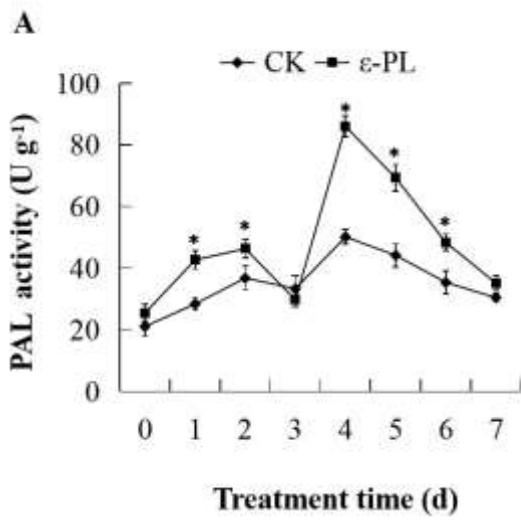
683

684 **Fig.5**

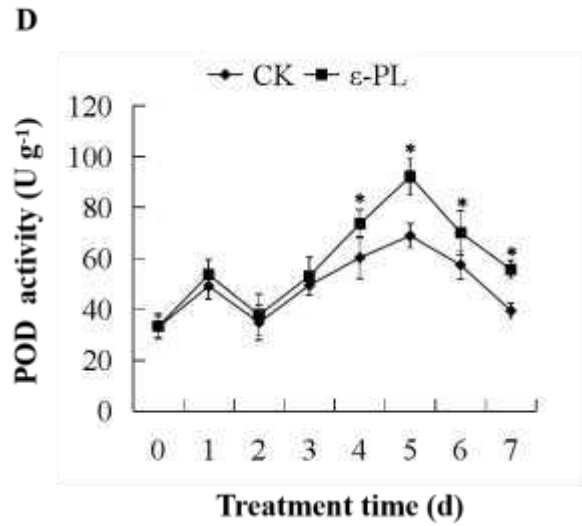
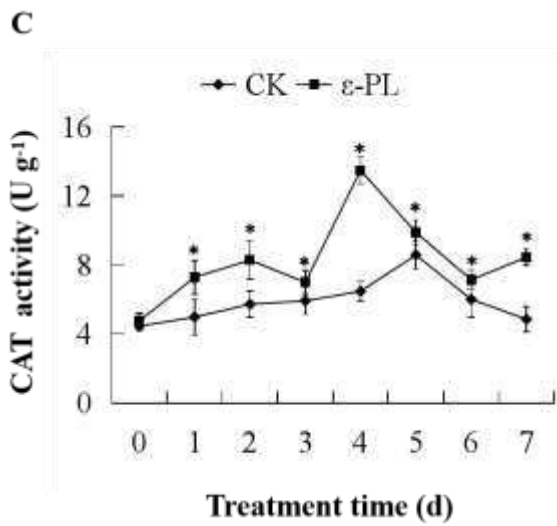


685

686 Fig.6



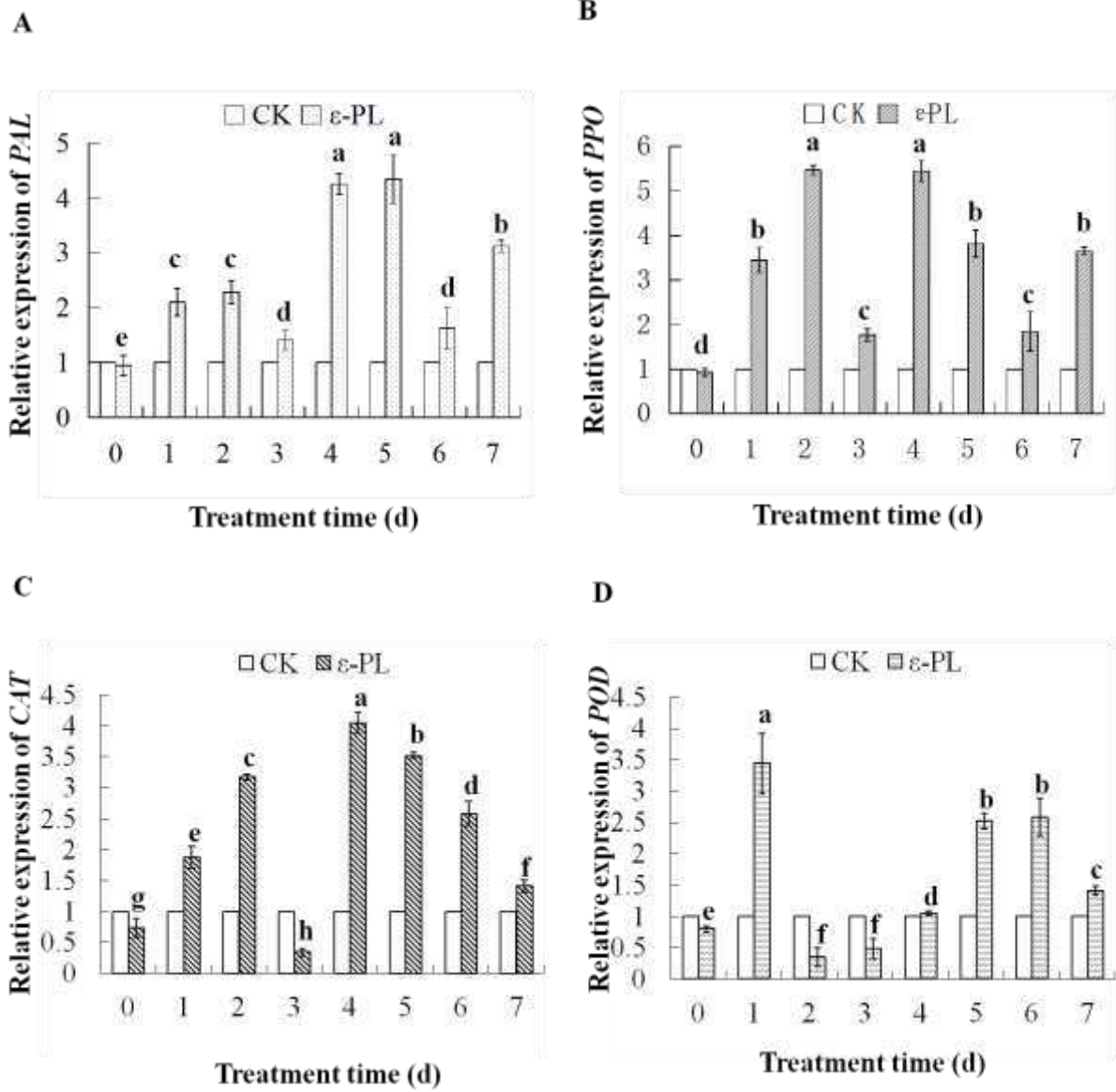
687



688

689

690 Fig.7



691

692

693